Neuroscience Research 149 (2019) 14–21

Contents lists available at ScienceDirect

Neuroscience Research

journal homepage: www.elsevier.com/locate/neures

Manganese-enhanced magnetic resonance imaging of the spinal cord in rats with formalin-induced pain

Myeounghoon Cha [a], Kyuhong Lee [b], Jun Sik Won [a], Bae Hwan Lee [a,c,*]

[a] Department of Physiology, Yonsei University College of Medicine, Seoul 03722, Republic of Korea
[b] Inhalation Toxicology Research Center, Korea Institute of Toxicology, Jeonbuk 56212, Republic of Korea
[c] Brain Korea 21 PLUS Project for Medical Science, Yonsei University College of Medicine, Seoul 03722, Republic of Korea

ARTICLE INFO

Article history:
Received 7 September 2018
Received in revised form 2 January 2019
Accepted 21 January 2019
Available online 24 January 2019

Keywords:
Manganese-enhanced MRI
Formalin induced pain
Pain imaging
Spinal cord
Spinothalamic tract

ABSTRACT

Manganese-enhanced magnetic resonance imaging (MEMRI) is based on neuronal activity-dependent manganese uptake, and provides information about nervous system function. However, systematic studies of pain processing using MEMRI are rare, and few investigations of pain using MEMRI have been performed in the spinal cord. Herein, we investigated the pain dependence of manganese ions administered in the rat spinal cord. $MnCl_2$ was administered into the spinal cord via an intrathecal catheter before formalin injection into the right hind paw (50 μL of 5% formalin). The duration of flinching behavior was recorded and analyzed to measure formalin-induced pain. After the behavioral test, rats were sacrificed with an overdose of urethane (50 mg/kg), and spine samples were extracted and post-fixed in 4% paraformaldehyde solution. The samples were stored in 30% sucrose until molecular resonance (MR) scanning was performed. In axial Mn^{2+} enhancement images of the spinal cord, Mn^{2+} levels were found to be significantly elevated on the ipsilateral side of the spinal cord in formalin-injected rats. To confirm pain-dependent Mn enhancement in the spinal cord, c-Fos expression was analyzed, and was found to be increased in the formalin-injected rats. These results indicate that MEMRI is useful for functional analysis of the spinal cord under pain conditions. The gray matter appears to be the focus of intense paramagnetic signals. MEMRI may provide an effective technique for visualizing activity-dependent patterns in the spinal cord.

1. Introduction

Magnetic resonance imaging (MRI) is a non-invasive imaging technology that produces detailed three-dimensional anatomical images without the use of damaging radiation (Bilgen et al., 2005; Bonny et al., 2008). Despite the intensive research on tracking and visualization techniques, studies that visually verify abnormal sensations, such as pain in the spinal cord have been challenging to perform due to technical difficulties. Since an effect of the manganese cation (Mn^{2+}) as a contrast agent has been observed in the earliest stages of MRI, Mn^{2+} is a useful paramagnetic contrast agent. The mechanism of action of Mn^{2+} is as a magnetic resonance (MR) contrast activity has been described (Pan et al., 2011). The chemical properties of Mn^{2+} resemble those of Ca^{2+}, and Mn^{2+} acts as a paramagnetic neuronal tract tracer because of its transport through voltage-gated Ca^{2+} channels throughout the nervous system (Pautler, 2004). Manganese-enhanced MRI (MEMRI) uses Mn^{2+} as a contrast agent, which shortens the spin-lattice relaxation time constant (T1) as Mn^{2+} enters the voltage-gated calcium channels of active neurons (Koretsky and Silva, 2004; Cha et al., 2016). Because of its characteristic features, Mn^{2+} can also be used as a track tracer to enable non-invasive in vivo visualization of functionally activated neural cells. Manganese can access neurons through voltage-gated L-type calcium channels and is transported anterograde using microtubule-based fast axonal transport (Pautler, 2004). Taken together, MEMRI is useful for visualizing functional neural activation and anatomy in the nervous system as an in vivo molecular imaging tracer. Furthermore, this tracer provides specific information about axonal integrity and facilitates the analysis and assessment of neuronal activation in response to noxious stimulation.

The most predictive acute pain model is the formalin-induced pain model (Dickenson and Sullivan, 1987; Martirosyan et al., 2010). Formalin-induced pain produces biphasic behavioral responses and abnormal behavior that lasts for approximately one

* Corresponding author at: Department of Physiology, Yonsei University College of Medicine, 50-1, Yonsei-ro, Seodaemun-gu, Seoul 03722, Republic of Korea.
E-mail address: bhlee@yuhs.ac (B.H. Lee).

https://doi.org/10.1016/j.neures.2019.01.007

hour. The behaviors include flinching, licking, biting, and shaking (Chang et al., 2012). The biphasic behavioral response consists of two different states. The first phase starts immediately after formalin injection and the second phase begins with increased abnormal behavior, after 10 min (Wheeler-Aceto et al., 1990). The first phase in the biphasic response is likely caused by direct tissue damage, and the second phase is due to peripheral inflammation and central sensitization (Shibata et al., 1989). The first and second phase responses that are induced by formalin have distinct characteristic properties, and this technique provides a useful method for examining the properties of inflammatory pain (Chang et al., 2014).

Current MEMRI studies have focused on visualizing neuronal connections and activation via Mn^{2+} administration (Freitag et al., 2015; Cha et al., 2016). MEMRI has been used to identify brain areas that are activated by noise exposure in mice (Walder et al., 2008) and image the retinal degeneration (Walder et al., 2008). Also, the neuronal alterations and activation have been observed in awake rabbits (Bilgen, 2006). MEMRI has also been used to study acute mesenteric ischemia and mesial temporal lobe epilepsy (Dedeurwaerdere et al., 2012; Zhao et al., 2015). These investigations indicate that MEMRI has the potential to reveal patterns and characteristics of neural activity. Although MEMRI provides functional information, the measurement of pain signaling in the spinal cord has only been attempted in a few studies (Martirosyan et al., 2010; Lei et al., 2014).

In our previous study, we collected rat brain MEMRI results after noxious electrical stimulation (Cha et al., 2016) and investigated c-Fos expression in the spinal cord upon acute inflammation pain using the formalin-induced pain model (Chang et al., 2012). We hypothesize that MEMRI may be an adequate imaging-based evaluation method for investigating changes in activated neuron after formalin-induced pain in the spinal cord. The purpose of this study was to investigate the correlation between the Mn^{2+}-enhancement and painful neuronal activity patterns in the spinal cord after formalin injection, and to examined the possibility of pain imaging using MEMRI.

2. Materials and methods

2.1. Animal preparation and intrathecal catheter implantation

Male Sprague-Dawley rats (250–300 g) were used in this experiment. Animals were housed in plastic cages with soft bedding on a 12 h light/dark cycle (light cycle: 08:00 ~20:00) and at a constant temperature ($22 \pm 2^\circ$) and humidity ($50 \pm 10\%$). All animal experiments were approved by the Institutional Animal Care and Use Committee of the Yonsei University Health System. Rats were anesthetized with an intraperitoneal injection of sodium pentobarbital (50 mg/kg). Deep anesthesia was verified by loss of nociception in response to tail pinch stimulation. The catheter polyethylene tubing (PE-10) was inserted caudally into the subarachnoid space of the rats through a small slit in the atlanto-occipital membrane and extended 7.5 cm beyond the slit. Each catheter was filled with heparin diluted saline (0.9% NaCl) before $MnCl_2$ injection. When the rats were fully alert and active, they were returned to their cages. Animals with suspected spinal cord injuries were excluded from the study.

2.2. $MnCl_2$ administration and formalin test

The formalin test was used to induce pain in these experiments (formalin n = 10, saline n = 10). Animals were placed in a plexiglass observation chamber ($46 \times 26 \times 20$ cm) and allowed to adapt for 10 min. After adaptation, $MnCl_2$ (10 mM of $MnCl_2$, 50 μl) solution was carefully injected via catheter. After injection, we waited for 5 min, to prevent leakage of $MnCl_2$ from the catheter. After $MnCl_2$ administration, 50 μL of 5% formalin was injected into the ventral surface of the left hind paw using a 29-gauge injection needle (Mojtahedin et al., 2008; Ortiz et al., 2008). The rat was placed in an observation chamber with a mirror that was mounted at a 45° angle beneath the floor, to allow an unobstructed view of the paw. The behaviors were recorded and used for analysis. The number of flinches in the injected paw was recorded as a measure of the nociceptive response and at 5 min intervals for 1 h. The recorded behaviors were divided into two phases: phase one was recorded between 0–10 min post-formalin injection (first phase), and phase two was recorded 10–60 min after post-formalin injection (second phase). After the formalin test, the rats were anesthetized with 25% urethane (1.25 g/kg, i.p.) that was perfused transcardially with normal saline, followed by 4% paraformaldehyde solution (in a 0.1 M PBS, pH 7.2). Catheters were then gently removed, and specimens were placed in 30% sucrose until ready for MR experiments. Finally, vertebrae and spinal cords (levels C6 to L6) were extracted and prepared for the c-Fos staining.

2.3. MR measurements

For the MR experiment, each vertebral column was inserted into a 50-mL polypropylene conical tube. The tubes were filled with formaldehyde solution to conserve the vertebra samples. Experiments were performed on a Biospec 4.7 T MRI system (Bruker BioSpin, Ettlingen, Germany) with a 40-cm diameter horizontal bore and a 72-mm sonator was used for emission and reception. Coronal and sagittal scouts were acquired using a RARE (Rapid Acquisition with Relaxation Enhancement) T2-weighted sequence. For analyzing the distribution of manganese ions, a set of noncontiguous T1-weighted (T1W) images was acquired that consisted of a spin-echo sequence using the following imaging parameters: TR = 500 ms, TE = 10 ms, 32 averages, slice thickness = 2 mm, field of view = 16×16 mm^2, matrix = 128×128, leading to a voxel size of 0.03 mm^3. Each slice was manually adjusted in the axial orientation of the scout images. The functional analysis was performed using ParaVision (Version 5.0, Bruker BioSpin). The spinal cord was outlined on axial slices, and the mean signal was calculated. To quantify data from the series of T1W images and measure Mn^{2+} enhancement in separated spinal regions, region of interests (ROIs) were set to the entire spinal cord regions that were covered in the coronal images. Six ROIs were manually drawn on each separate image, including the ipsilateral and contralateral side of dorsal (laminae I—II), intermediate (laminae III-VI), and ventral parts (laminae VII–X). The mean intensity was defined as the average of signal intensity at each ROI in the groups. The mean intensity in the paravertebral ROIs were used to calculate the normalized Mn^{2+} signal intensities. Image analysis was performed using ParaVision (Bruker Biospin), MRVision (MRVision Co., Winchester, MA, US) and ImageJ software (NIH, Bethesda, MD, US).

2.4. c-Fos immunohistology

After MR imaging, each spinal cord tissue was embedded into OCT medium (TissueTek, Torrance, CA, USA), quick frozen, and stored in a deep freezer until further processing. To verify neuronal activation in the spinal cord, c-Fos expression in the spinal cord of saline and formalin-injected rats was observed as a marker of neuronal activation. Immunohistochemistry protocols were described previously (Cha et al., 2017). Frozen sections (12 μm) of the spinal cord were prepared using a cryostat (HM500, Microm, Walldorf, Germany). To visualize c-Fos, the sections were incubated overnight at 4 °C with c-Fos anti-rabbit polyclonal IgG (1:250, Santa Cruz Biotechnology, Santa Cruz, CA, US). Then, the sections were washed with PBS and further incubated for 2 h at room tempera-

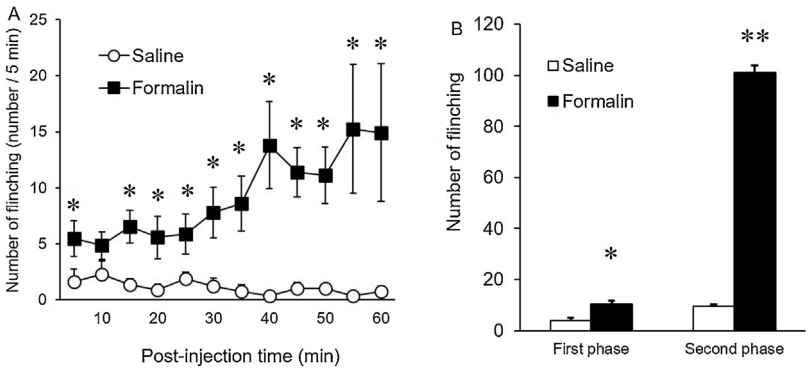

Fig. 1. Behavioral test for formalin-induced pain. A) Time dependent changes of flinching behaviors (*p < 0.05 compared to saline-injected group (mean and standard deviation). B) Biphasic formalin-induced flinching behavior was analyzed. The first and second phase of formalin data were compared to the saline group (one-way ANOVA). Data are expressed as the mean number of flinches per min ± SEM for each animal (*p < 0.05 and **p < 0.01).

ture with Alexa Fluor 488. Each section in the T11-L6 segments of the spinal cord from individual experimental animals was divided equally on MR imaging (laminae I–II, III–VI and VI–X regions). The number of c-Fos-positive neurons was observed and captured under a 40X microscope (Olympus BX51 microscope, Tokyo, Japan) mounted with a CCD camera (Cool SNAP, Photometrics, Tucson, AZ, US). ImageJ software was used to count c-Fos positive neurons.

2.5. Statistical analysis

Flinching behavior results were presented as mean ± standard error of the mean (SEM) and were assessed using the SPSS program (SPSS Ver. 22.0, SPSS Inc., Chicago, IL, US). Differences in the flinching frequencies during early and late phase responses were analyzed by one-way ANOVA followed by Dunnett's post-hoc pairwise comparison. In the MR imaging, the signal magnitudes from each spinal cord region were normalized to the signal intensity in the temporalis muscle. Results of the Mn-enhanced signals were compared by a nonparametric analysis that included the Friedman test for within-group comparisons and the Kruskal–Wallis test for between-group comparisons. Multiple comparisons after the Friedman test and Kruskal–Wallis test were performed using Dunnett's test for nonparametric analysis. For c-Fos analysis, the numbers of c-Fos positive neurons were compared using the same statistical method mentioned above. A p value of less than 0.05 was considered statistically significant.

3. Results

3.1. Behavioral test

After 5% formalin injection into the plantar surface of the left hind paw, the rats showed flinching behaviors. These responses were separated into first and second phase responses. We classified rats into two groups (saline and 5% formalin injection groups). The frequencies of the flinching behavior in the first and second

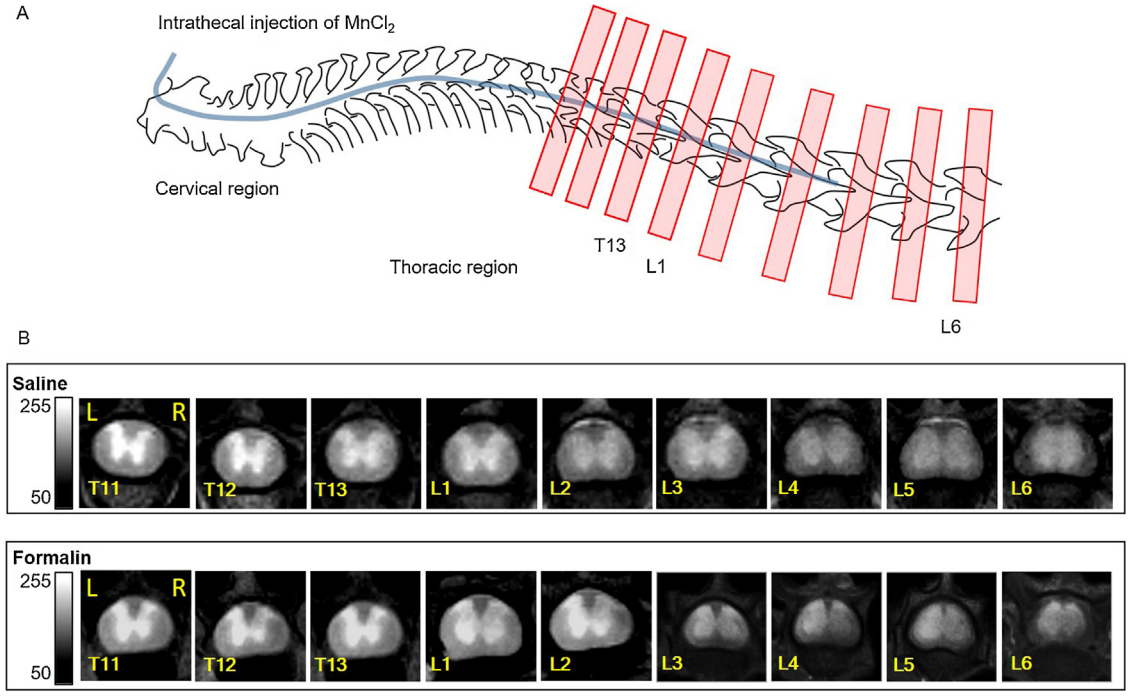

Fig. 2. Diagram of formalin injection route. A) Nine axial slice (red boxes) positions indicate the acquired Mn-enhanced MR imaging scans. The curved blue line shows the $MnCl_2$ injection route via polyethylene tube (PE-10). The end of the catheter was located between the L2–L4 levels of the spinal cord. B) Mn enhanced images we acquired from each rat of the experimental group. Rostro-caudal sequences of T1-weighted coronal images of saline- or formalin-injected rat spinal cords were acquired for further analysis (For interpretation of the references to colour in this figure legend, the reader is referred to the web version of this article).

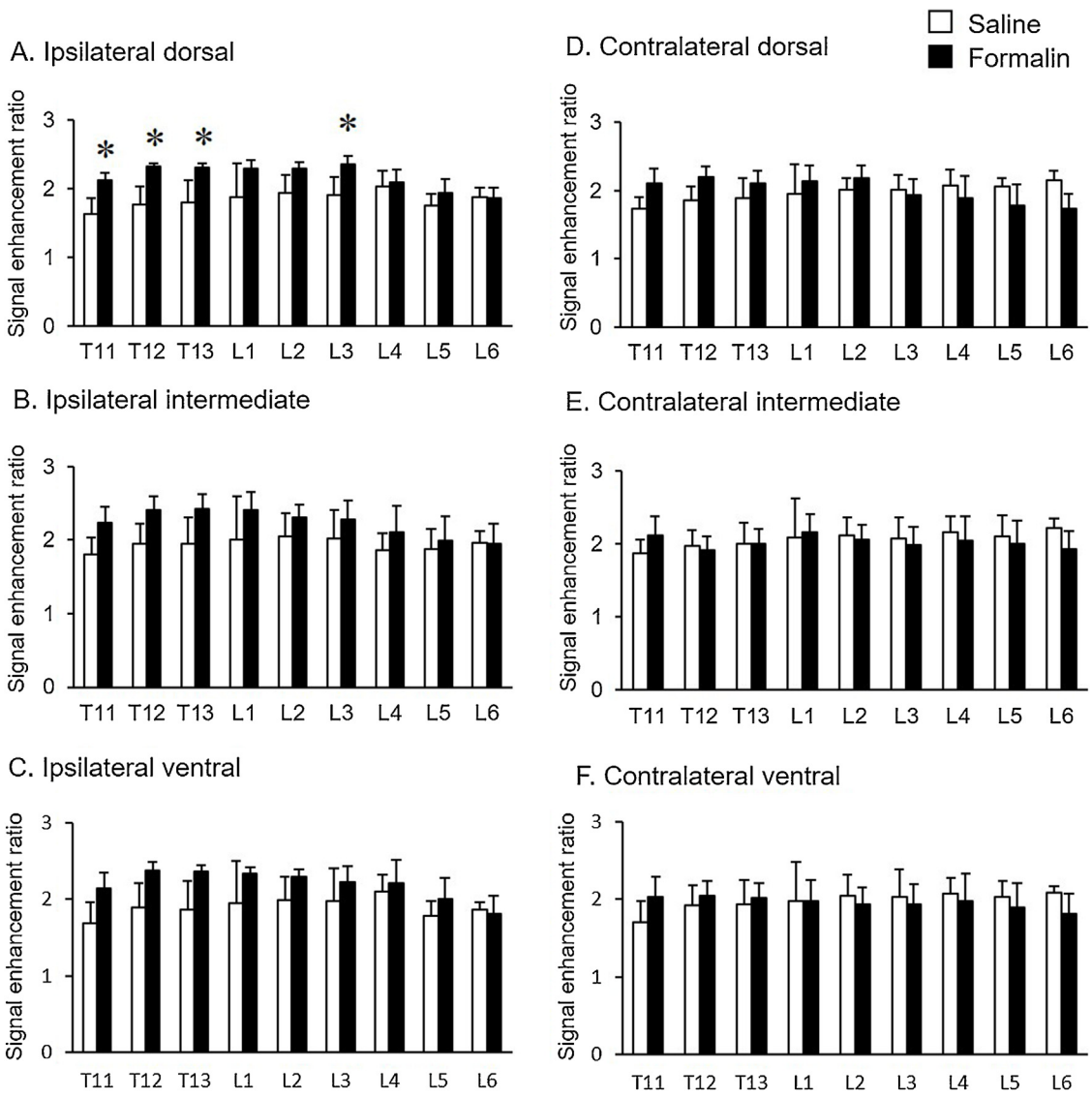

Fig. 3. Laminae-dependent Mn^{2+} enhancements in the spinal cord. Region of interest (ROI) analysis of signal enhancement was performed. Six regions of Mn-enhanced signal intensity in MR images were compared and analyzed. Signal intensity of the ipsilateral part of formalin-injected rats showed higher intensity compared to that of saline-injected rats (A) ipsilateral dorsal, B) intermediate and C) ventral region, *p < 0.05). However, signal intensity of the contralateral side (D–F) did not show significant differences (nonparametric analysis used).

phases were counted. As shown in Fig. 1, the number of flinching behaviors in formalin-injected rats significantly increased compared to saline-injected rats during the recording period ($p < 0.05$, Fig. 1A). The total recording time was divided into the first and second phases for phase analysis (Fig. 1B). The number of flinches in the saline injection group were 2.06 ± 1.17 and 5.11 ± 2.35 in the first and second phases, respectively. However, the number of flinches in 5% formalin-injected rats were 10.33 ± 2.49 and 100.933 ± 25.6 in the first and second phases, respectively. These data show that formalin injection significantly increases flinching behavior during the first and second phases compared to saline injection.

3.2. Comparison of manganese-enhanced MR signals

MR images were acquired with different adjustments, in consideration of the specific bending of the vertebrae. Nine red rectangles with vertebrae indicate the simplified position of the acquired plane that was used for Mn-enhanced MR imaging (Fig. 2A). The curved thick blue line indicates the $MnCl_2$ injection route using the catheter. The Mn^{2+} uptake in the spinal cord appeared after intrathecal $MnCl_2$ injections as brightened T1-weighted signals from the entire spinal cord. A total of 16 axial images were obtained from the cervical, thoracic, lumbar, and upper sacral levels and the thoracic eleventh to the lumbar sixth levels were selected for imaging analysis (Fig. 2B). In the gray matter of the spinal cord, strong Mn^{2+} signal enhancements were observed compared with the saline group, although this difference was not significant. However, the formalin group showed differences between ipsilateral and contralateral sides, and laminae-dependent changes in the lumbar levels. This finding indicates that Mn^{2+} uptake into functionally active neuronal tissue after formalin injection allows analysis of the spinal cord. Furthermore, the Mn-enhanced axial spinal cord images showed the typical anatomical structure of the spinal cord and differentiated between gray and white matter, as expected.

For a precise comparison, we divided the gray matter into six parts at each spinal cord image (dorsal, intermediate, and ventral parts of the ipsilateral and contralateral sides). The signal

enhancement ratio of each region was calculated by a ratio of signal intensity in the region of interest (ROI) divided by the signal intensity at a reference region. The increased Mn^{2+} enhancements from the entire level of the spinal cord were compared in terms of the signal enhancement ratio of the ipsilateral and contralateral side. In the comparison of ipsilateral and contralateral side Mn^{2+} enhancements in formalin-injected rats, the signal intensities of the ipsilateral sides were higher (Fig. 3A and D, B and E, and C and F). Specifically, at the thoracic eleventh to thirteenth and the lumbar third level of the ipsilateral dorsal region, the signal enhancements were much higher than those of the ipsilateral dorsal region in saline-injected rats (Fig. 3A). However, the ipsilateral intermediate and ventral regions did not show significant differences (Fig. 3B and C). In saline-injected rats, Mn^{2+} enhancement signals were elevated at both sides and did not show significantly increased or decreased intensities. The saline-injection also elevated the signal intensity, which could be explained by the general uptake of Mn^{2+}.

3.3. Comparison of Mn^{2+} enhancement between ipsilateral and contralateral sides

In our analysis, the saline-injected rats did not show significant changes in ipsilateral/contralateral ROIs ratios at all spinal levels. However, the comparison ratio at the dorsal region of the lumbar third level in the formalin-injection rats was significantly higher than that of the other levels (Fig. 4A, $^*p < 0.05$). Also, at the intermediate region, the intensity ratios at the lumbar second and third showed significant changes (Fig. 4B). Finally, the ventral region showed significantly enhanced signal ratios, from the thoracic thirteenth to the lumbar third level (Fig. 4C). The result of the contrast enhancements in the ventral regions indicates that the flinching behavior in the formalin model is reflected by the Mn-enhanced signals in the spinal cord. Furthermore, the small differences between saline- and formalin-injected rats in the upper level suggests that Mn evenly enhanced the spinal cord without ipsilateral/contralateral differences.

3.4. c-Fos expression in the spinal cord

The number of c-Fos positive neurons in the spinal cord were observed separately for the dorsal part (laminae I—II), intermediate region (III–VI), and ventral area (VI—X). All c-Fos positive neurons were counted and calculated using ipsilateral/contralateral ratio. To compare MEMRI images with traditional immunohistochemistry patterns, we compared c-Fos expression from T13 to L4, which showed a significant change on MEMRI. Representative images of c-Fos positive neurons in the spinal cord of the saline- and formalin-injected rats are shown in Fig. 5: The dorsoventral and ipsi-contra axes are shown in Fig. 5A (left). As seen in Fig. 5A (middle), few c-Fos positive neurons appeared at level L3 of spinal cords from saline-injected rats. However, at the same level in formalin-injected rats, remarkable increases in c-Fos positive neurons were found at the dorsal, intermediate, and ventral regions of the spinal cord, compared to the saline-injected rats (Fig. 5A, right). Comparison of c-Fos expression in saline and formalin rats is shown in Fig. 5B. The difference between ipsilateral and contralateral parts was noticeable in the dorsal portions of levels L2 and L3. However, other regions had no significant difference. Counting analysis of c-Fos positive cells is shown in Fig. 6. The c-Fos positive neurons were counted and graphed in the dorsal, intermediate, and ventral regions of laminae. In the formalin group, a very significant increase was observed in dorsal L2 and L3 regions (Fig. 6A, $^*p < 0.05$).

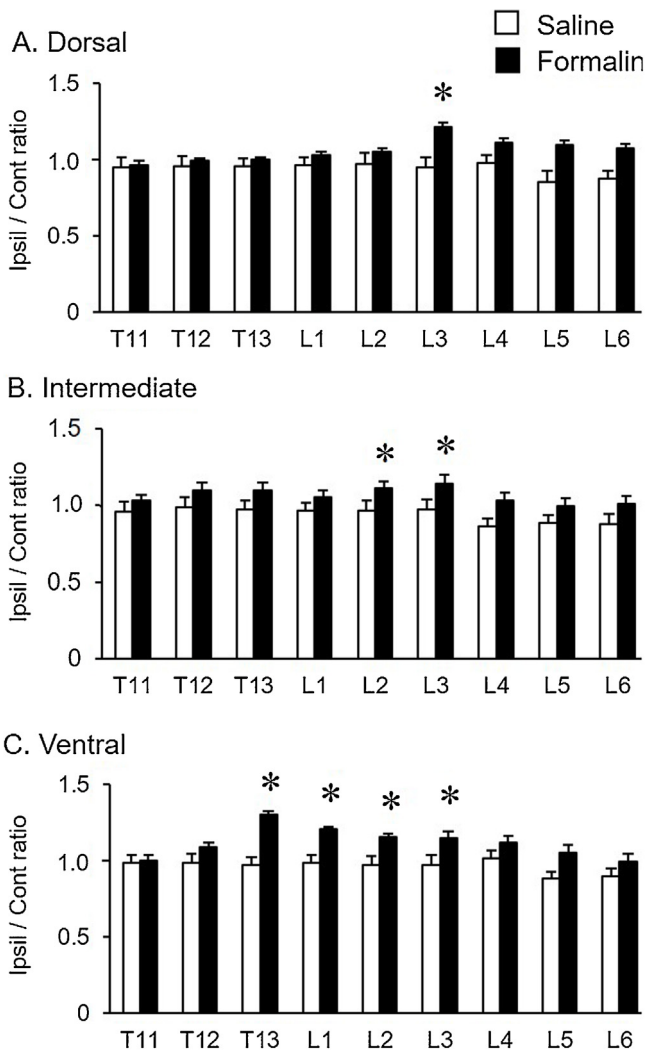

Fig. 4. Signal intensity ratio of the ipsilateral/contralateral side of the spinal cord. Signal intensity of the ipsi/cont ratio was analyzed at A) dorsal, B) intermediate, and C) ventral parts of the spinal cord. Mn-enhanced signal intensity was measured by the ratio of ipsi/cont signals of each MR image. The formalin-injected rats showed higher signal intensity ratios compared with saline-injected rats (dorsal: L3, intermediate: L2 and L3, and ventral: T13, L1, L2, and L3). ($^*p < 0.05$. Nonparametric analysis used, data are presented as mean ± SEM).

4. Discussion

The present study shows the Mn^{2+} enhancement is related to signal transduction in the spinal cord. Also these findings suggest that manganese preferably accumulates in excited neuronal cells/axons, and inactivated neurons show less contrast enhancement, which is a sign of less manganese enhancement in these neuronal cells. Therefore, our behavioral assessment rating and immunohistological results support that Mn^{2+} concentrations correlate with noxious pain signaling in the spinal cord. Taking the above evidence as the basis for our current study, we conclude that MEMRI is an adequate tool for monitoring signal transduction in the spinal cord.

4.1. The meaning of Mn^{2+} enhancement in the spinal cord

The remarkable Mn^{2+} enhancement in the thoracic and lumbar levels in formalin-injected animals suggests that Mn^{2+} enhancement is highly related to neural cells and axonal activation. This idea is supported by previous studies that showed that evoked

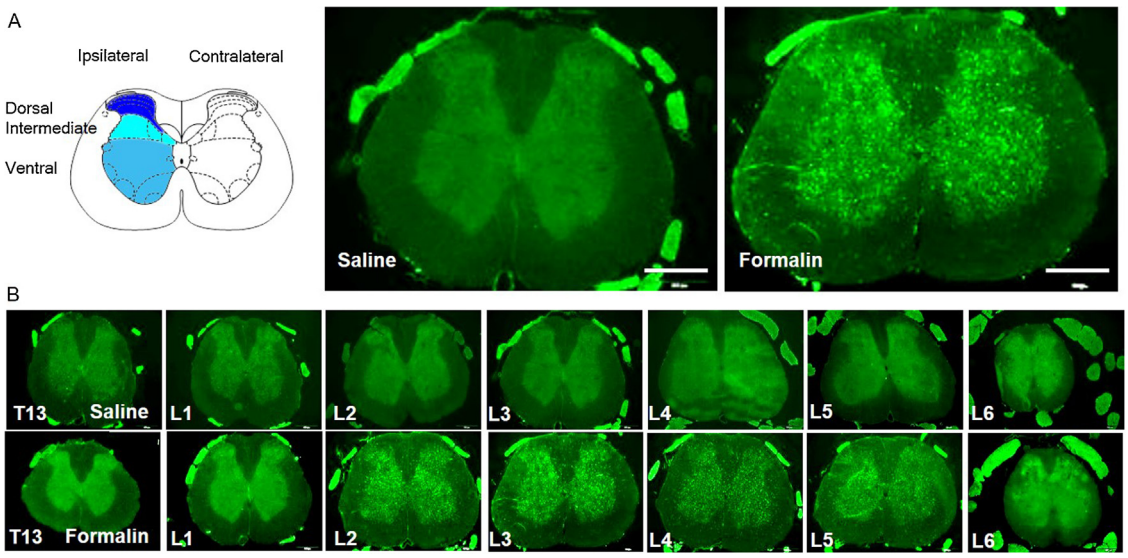

Fig. 5. Comparison of c-Fos positive expressions in the spinal cord. A) Representative images of c-Fos expression in L3 level of saline and formalin-injected groups are shown. The number of c-Fos-positive neurons was counted at dorsal, intermediate, and ventral parts of the ipsilateral and contralateral sides in the spinal cord. Higher c-Fos expression was observed in formalin-injected rats. B) The level dependent comparison of c-Fos positive neuron comparison. Expression of c-Fos-positive neurons in different groups were compared. (Scale bar = 500 um).

neuronal activity appeared when subjects were exposed formalin-induced pain (Dickenson and Sullivan, 1987; Kaneko et al., 2000; Barr, 2011). The main advantage of using MRI methods is to visualize status changes in vivo. In this study, we attempted to observe changes in formalin-induced neuronal activity in tissues extracted *ex vivo*, since *ex vivo* imaging benefits from greater resolution and sensitivity due to the lack of constraints on imaging time, use of tighter fitting coils, high concentration contrast agents, and a lack of movement artifacts (Mackenzie-Graham, 2012). These advantages make it possible to identify the grade and extent of pain more accurately and quickly than using traditional methods. In this study, we were able to observe high-resolution images in the spinal cord and analyze the data. Our findings show that Mn^{2+} enhancement in the ipsilateral side after formalin injection into the hind paw significantly increased signal intensity. This could suggest that the Mn^{2+} enhancement was highly correlated with the formalin-induced nociceptive input. Nevertheless, the next question is "what causes the Mn^{2+} enhancement in the control rats: enhanced tactile input or spontaneous activity in the peripheral or central nervous system?" After saline injection into control rats, they showed normal behavior, such as exploring, grooming, and flinching. These behaviors could contribute to neural activation in the spinal cord. These unexpected enhanced signal contributions may affect spontaneous neural activity after routine behavior, and several types of evidence support this idea. Single- and multi-unit neuronal studies in nerve-injured rodents have found heightened touch-evoked activity and increased spontaneous discharge in neurons in the spinal cord dorsal horn (Laird and Bennett, 1993) and primary somatosensory cortex (Ochoa et al., 2005; Defrin et al., 2015). In Fig. 3, we first compared the Mn-enhanced patterns between two groups, saline and formalin-injected rats, since we needed to confirm the spontaneous neuronal activity in the spinal cord after saline injection. As shown in Fig. 3A, Mn-enhanced patterns were significantly higher in ipsilateral dorsal parts of the formalin injection group. This indicated formalin-induced pain in the spinal cord. However, this comparison could not eliminate Mn-enhanced patterns produced by spontaneous behavioral activities, such as walking and grooming. For this reason, an alternative analysis was required for Fig. 4, in which we compared the Mn-enhanced contralateral-to-ipsilateral ratio of each spinal axial image from the same animals. This analysis could be used to distinguish the actual neuronal activities by formalin-induced pain from those produced by spontaneous behaviors. Although the MR signal intensity did not significantly increase at the whole level of the spinal cord in formalin–injected rats, the significant difference that was observed in the ipsilateral dorsal parts could indicate formalin-induced pain.

4.2. Does Mn^{2+} enhancement in the spinal cord suggest peripherally transduced acute formalin-induced pain?

Recent spine studies with Mn^{2+} enhanced MRI have focused on neuronal damage after experimental spinal cord injury (Martirosyan et al., 2010; Matsuda et al., 2010; Freitag et al., 2015). These studies found statistically significant correlations among the MR signal intensity, the behavioral functional test, and the retrograde axonal tracing. MEMRI could allow compatible pain research, although it has not yet been actively examined due to technical limitations. The previously reported Mn^{2+} enhanced MR imaging studies have shown only weak labeling of the spinothalamic tract (Bilgen, 2006; Walder et al., 2008). In the present study, we examined the enhancement changes of the spinal cord following injection of saline or formalin into the hind paw after $MnCl_2$ injection into the spinal space using a suitable concentration of MEMRI. Direct subarachnoidal injection of $MnCl_2$ has the advantage of producing stronger labeling of the spinothalamic tract, especially in the spinal cord. Our data show the feasibility of tracing the spinothalamic tract using Mn^{2+} alone and suggest that formalin-induced acute nociceptive sensations are reflected in the spinothalamic tract by the sensitivity and specificity of Mn^{2+} ions. In addition, laminar-dependent analysis indicated pain-related signals at dorsal parts of the spinal cord. The dorsal region is a superficial layer that is involved in pain processing. However, Mn-enhanced signals may involve neuronal activity in the spinal cord, induced by spontaneous behaviors. Therefore, we additionally analyzed pain-induced signals using ipsilateral/contralateral ratio (Fig. 4). This enhanced labeling is most likely a consequence of a stimulation-induced increase in activity of spinothalamic tract, which increases the uptake and anterograde transport of Mn^{2+} ions.

In Fig. 6, we compared and analyzed c-Fos immunoreactivity in the spinal cords of saline and formalin-injected rats. The results of

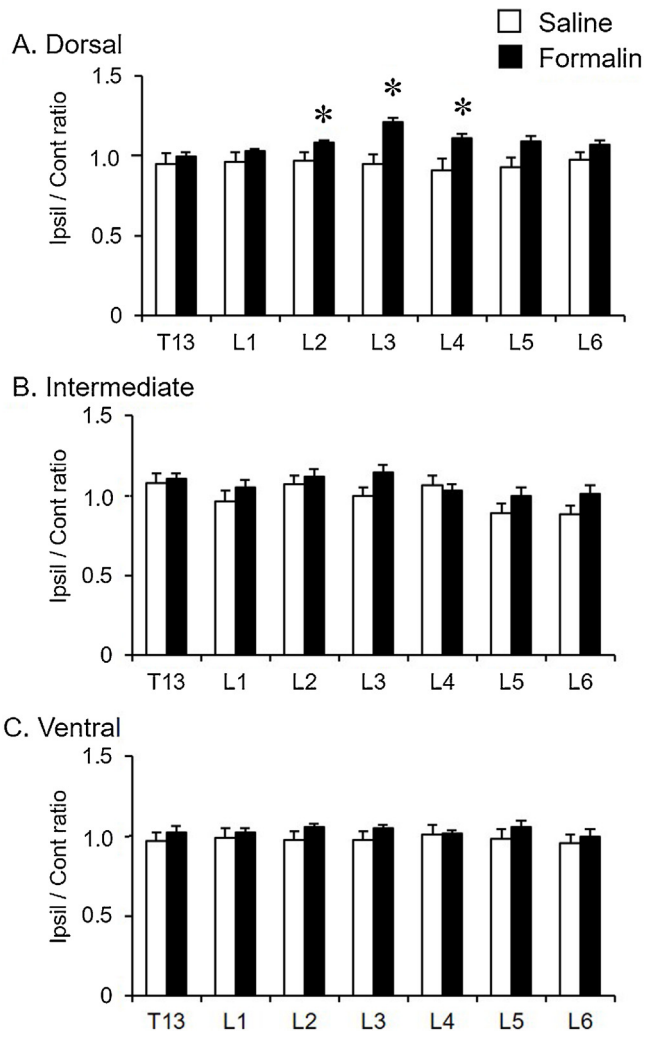

Fig. 6. C-fos expression ratio of the ipsilateral/contralateral side of the spinal cord. C-fos expression of the ipsi/cont ratio was analyzed at A) dorsal, B) intermediate, and C) ventral parts of the spinal cord T13 to L6 levels. The formalin-injected rats showed higher c-fos expression ratios compared with saline-injected rats (dorsal: L2–L4). ($^{*}p < 0.05$, data are presented as mean ± SEM).

our c-Fos expression experiments showed that formalin-induced pain could be expressed in dorsal parts of the spinal cord. According to previous studies, the most extensive labeling is generated by noxious stimuli in regions of the dorsal horn that receive small diameter primary afferents, including Aδ and C fibers (D'Mello and Dickenson, 2008; Basbaum et al., 2009). In addition, the involved regions are laminae I, II, and lamina V in some cases (Todd, 2010; Steeds, 2016). These results were consistent with those of previous studies (Yi and Barr, 1997; Laudanna et al., 1998). However, in the comparison of MEMRI with conventional methods, significantly higher expressions of c-Fos were not observed in intermediate and ventral sides of the spinal cord. In comparison, Mn-enhanced signals could present neuronal activities upon painful sensation. Furthermore, using conventional methods, differences between saline and formalin-injected rats were observed only at the dorsal part of lumbar levels 2 and 3. This suggests that Mn-enhanced signals may include neuronal activities produced by spontaneous behaviors.

The present results indicate that MEMRI could be useful for functional studies of the spinal cord under pain conditions. Moreover, these results suggest that the gray matter is the foci of intense paramagnetic signals, and MEMRI may provide an effective technique to visualize activity-dependent patterns in the spinal cord.

Statement of interests

The authors declare that there are no conflicts of interest regarding the publication of this paper.

Acknowledgements

This study was supported by the Basic Research Program through the National Research Foundation (NRF) and funded by the Ministry of Science, ICT & Future Planning (NRF-2015R1C1A1A01053484 and 2017R1A2B3005753).

References

Barr, G.A., 2011. Formalin-induced c-fos expression in the brain of infant rats. J. Pain 12, 263–271.
Basbaum, A.I., Bautista, D.M., Scherrer, G., Julius, D., 2009. Cellular and molecular mechanisms of pain. Cell 139, 267–284.
Bilgen, M., 2006. Imaging corticospinal tract connectivity in injured rat spinal cord using manganese-enhanced MRI. BMC Med. Imaging 6, 15.
Bilgen, M., Dancause, N., Al-Hafez, B., He, Y.Y., Malone, T.M., 2005. Manganese-enhanced MRI of rat spinal cord injury. Magn. Reson. Imaging 23, 829–832.
Bonny, J.M., Mailly, P., Renou, J.P., Orsal, D., Benmoussa, A., Stettler, O., 2008. Analysis of laminar activity in normal and injured rat spinal cord by manganese enhanced MRI. Neuroimage 40, 1542–1551.
Cha, M., Lee, K., Lee, C., Cho, J.H., Cheong, C., Sohn, J.H., Lee, B.H., 2016. Manganese-enhanced MR imaging of brain activation evoked by noxious peripheral electrical stimulation. Neurosci. Lett. 613, 13–18.
Cha, M., Um, S.W., Kwon, M., Nam, T.S., Lee, B.H., 2017. Repetitive motor cortex stimulation reinforces the pain modulation circuits of peripheral neuropathic pain. Sci. Rep. 7, 7986.
Chang, K.H., Won, R., Shim, I., Lee, H., Lee, B.H., 2012. Effects of electroacupuncture at BL60 on formalin-induced pain in rats. Evid. Complement. Alternat. Med. 2012, 324039.
Chang, K.H., Bai, S.J., Lee, H., Lee, B.H., 2014. Effects of acupuncture stimulation at different acupoints on formalin-induced pain in rats. Korean J. Physiol. Pharmacol. 18, 121–127.
D'Mello, R., Dickenson, A.H., 2008. Spinal cord mechanisms of pain. Br. J. Anaesth. 101, 8–16.
Dedeurwaerdere, S., Fang, K., Chow, M., Shen, Y.T., Noordman, I., van Raay, L., Faggian, N., Porritt, M., Egan, G., O'Brien, T., 2012. Manganese-enhanced MRI reflects seizure outcome in a model for mesial temporal lobe epilepsy. NeuroImage 68, 30–38.
Defrin, R., Amanzio, M., de Tommaso, M., Dimova, V., Filipovic, S., Finn, D.P., Gimenez-Llort, L., Invitto, S., Jensen-Dahm, C., Lautenbacher, S., Oosterman, J.M., Petrini, L., Pick, C.G., Pickering, G., Vase, L., Kunz, M., 2015. Experimental pain processing in individuals with cognitive impairment: current state of the science. Pain 156, 1396–1408.
Dickenson, A.H., Sullivan, A.F., 1987. Subcutaneous formalin-induced activity of dorsal horn neurones in the rat: differential response to an intrathecal opiate administered pre or post formalin. Pain 30, 349–360.
Freitag, M.T., Marton, G., Pajer, K., Hartmann, J., Walder, N., Rossmann, M., Parzer, P., Redl, H., Nogradi, A., Stieltjes, B., 2015. Monitoring of short-term erythropoietin therapy in rats with acute spinal cord injury using manganese-enhanced magnetic resonance imaging. J. Neuroimaging 25, 582–589.
Kaneko, M., Mestre, C., Sánchez, E.H., Hammond, D.L., 2000. Intrathecally administered gabapentin inhibits formalin-evoked nociception and the expression of fos-like immunoreactivity in the spinal cord of the rat. J. Pharmacol. Exp. Ther. 292, 743–751.
Koretsky, A.P., Silva, A.C., 2004. Manganese-enhanced magnetic resonance imaging (MEMRI). NMR Biomed. 17, 527–531.
Laird, J.M., Bennett, G.J., 1993. An electrophysiological study of dorsal horn neurons in the spinal cord of rats with an experimental peripheral neuropathy. J. Neurophysiol. 69, 2072–2085.
Laudanna, A., Nogueira, M.I., Mariano, M., 1998. Expression of Fos protein in the rat central nervous system in response to noxious stimulation: effects of chronic inflammation of the superior cervical ganglion. Braz. J. Med. Biol. Res. 31, 847–850.
Lei, B.H., Chen, J.H., Yin, H.S., 2014. Repeated amphetamine treatment alters spinal magnetic resonance signals and pain sensitivity in mice. Neurosci. Lett. 583, 70–75.
Mackenzie-Graham, A., 2012. In vivo vs. ex vivo magnetic resonance imaging in mice. Front. Neuroinform. 6, 19-19.
Martirosyan, N.L., Bennett, K.M., Theodore, N., Preul, M.C., 2010. Manganese-enhanced magnetic resonance imaging in experimental spinal cord injury: correlation between T1-weighted changes and Mn(2+) concentrations. Neurosurgery 66, 131–136.

Matsuda, K., Wang, H.X., Suo, C., McCombe, D., Horne, M.K., Morrison, W.A., Egan, G.F., 2010. Retrograde axonal tracing using manganese enhanced magnetic resonance imaging. Neuroimage 50, 366–374.
Mojtahedin, A., Tamaddonfard, E., Zanboori, A., 2008. Antinociception induced by central administration of histamine in the formalin test in rats. Indian J. Physiol. Pharmacol. 52, 249–254.
Ochoa, J.L., 2005. Comment on: a role for the brainstem in central sensitization in humans. evidence from functional magnetic resonance imaging. Pain 117, author reply 236–237, Zambreanu et al. Pain 2005; 114: 397–407.
Ortiz, M.I., Lozano-Cuenca, J., Granados-Soto, V., Castaneda-Hernandez, G., 2008. Additive interaction between peripheral and central mechanisms involved in the antinociceptive effect of diclofenac in the formalin test in rats. Pharmacol. Biochem. Behav. 91, 32–37.
Pan, D., Schmieder, A.H., Wickline, S.A., Lanza, G.M., 2011. Manganese-based MRI contrast agents: past, present and future. Tetrahedron 67, 8431–8444.
Pautler, R.G., 2004. In vivo, trans-synaptic tract-tracing utilizing manganese-enhanced magnetic resonance imaging (MEMRI). NMR Biomed. 17, 595–601.
Shibata, M., Ohkubo, T., Takahashi, H., Inoki, R., 1989. Modified formalin test: characteristic biphasic pain response. Pain 38, 347–352.
Steeds, C.E., 2016. The anatomy and physiology of pain. Surgery - Oxford International Edition 34, 55–59.
Todd, A.J., 2010. Neuronal circuitry for pain processing in the dorsal horn. Nat. Rev. Neurosci. 11, 823–836.
Walder, N., Petter-Puchner, A.H., Brejnikow, M., Redl, H., Essig, M., Stieltjes, B., 2008. Manganese enhanced magnetic resonance imaging in a contusion model of spinal cord injury in rats: correlation with motor function. Invest. Radiol. 43, 277–283.
Wheeler-Aceto, H., Porreca, F., Cowan, A., 1990. The rat paw formalin test: comparison of noxious agents. Pain 40, 229–238.
Yi, D.K., Barr, G.A., 1997. Formalin-induced c-fos expression in the spinal cord of fetal rats. Pain 73, 347–354.
Zhao, D., Cheng, C., Kuang, L., Zhang, Y., Cheng, H., Min, J., Wang, Y., 2015. A new approach using manganese-enhanced MRI to diagnose acute mesenteric ischemia in a rabbit model: initial experience. Biomed Res. Int. 2015.